BMC Infectious Diseases

RESEARCH

Open Access

A novel malaria mathematical model: integrating vector and non-vector transmission pathways

Emmanuel Akowe[1], Queeneth Ojoma Ahman[1*], Benedict Celestine Agbata[1], Solomon Onuche Joseph[1], Emmanuel Olorunfemi Senewo[1], Abdul Yusuf Danjuma[2] and Danjuma Jibrin Yahaya[1]

Abstract

Background Malaria remains one of the most significant global health challenges, particularly in tropical and sub-tropical regions. Despite ongoing control efforts, malaria transmission persists due to complex biological, environmental, and socio-economic factors. Traditional malaria models have primarily focused on vector-borne transmission, overlooking the growing importance of non-vector transmission pathways, such as blood transfusions, congenital transmission, and human-to-human transmission through healthcare settings.

Methods A novel mathematical model was developed to integrate both vector-borne and non-vector transmission routes. The model expands the traditional Susceptible-Exposed-Infectious-Recovered (SEIR) framework by incorporating compartments for vaccinated and non-vector exposed human populations, as well as dynamics for both human and mosquito populations. Numerical simulations were performed using MATLAB to evaluate the impact of vaccination, vector control, non-vector control, and treatment strategies.

Results The results indicate that vaccination significantly reduces susceptibility to malaria, with numerical simulations showing an approximate 43% reduction in the susceptible human population. However, vector control remains critical in limiting exposure, and non-vector transmission pathways including blood transfusions, congenital transmission, and direct human-to-human transmission pose a substantial risk even in regions with effective mosquito control. This underscores the need for integrated strategies that address both vector and non-vector transmission routes.

Conclusions Combining vaccination efforts with robust vector control, improved healthcare practices, and stringent non-vector transmission prevention measures is essential to effectively reduce malaria transmission. Sustained interventions, including improved blood screening and safe medical practices, are necessary to prevent malaria resurgence, particularly in high-transmission settings. This model provides valuable insights into malaria dynamics and offers a framework for designing more effective public health policies and strategies for malaria eradication.

Keywords Malaria transmission dynamics, Vector transmission, Non-vector transmission, SEIR model, Mathematical modeling

*Correspondence:
Queeneth Ojoma Ahman
ahmanqo@custech.edu.ng
[1] Department of Mathematics/Statistics, Confluence University of Science and Technology, Osara, Kogi State, Nigeria
[2] Department of Actuarial Science, Confluence University of Science and Technology, Osara, Kogi State, Nigeria

Background

Malaria continues to be one of the most significant global health challenges, causing extensive morbidity and mortality worldwide. According to the World Health Organization (WHO), malaria caused over 247 million cases and 619,000 deaths globally in 2021, with the majority

of cases concentrated in sub-Saharan Africa. Vulnerable populations, including young children and pregnant women, are disproportionately affected, further exacerbating existing health inequities[1]. Malaria is caused by protozoan parasites of the genus *Plasmodium*, primarily transmitted through the bites of infected female *Anopheles* mosquitoes [2]. Despite the significant progress achieved through interventions such as insecticide-treated nets (ITNs), indoor residual spraying (IRS), and antimalarial medications, malaria persists due to its complex transmission dynamics and the interplay of biological, environmental, and socio-economic factors [3, 4].

Malaria has traditionally been understood as a vector-borne disease, with *Anopheles* mosquitoes playing the primary role in its transmission [5, 6]. Mathematical models, particularly those employing the Susceptible-Exposed-Infectious-Recovered (SEIR) framework, have been instrumental in simulating the interactions between human and mosquito populations, offering insights into the dynamics of disease spread and the impact of control strategies [7]. These models have guided interventions such as insecticide-treated nets (ITNs), indoor residual spraying (IRS), and antimalarial medications, which have significantly reduced transmission rates in many endemic regions [4, 8]. However, this vector-centric approach, while effective, overlooks other important pathways through which malaria is transmitted.

Non-vector transmission routes, including blood transfusions, congenital transmission, and organ transplants, have been increasingly recognized as critical contributors to malaria persistence in specific contexts [9, 10]. For instance, in areas where mosquito control measures are successful, the risk of malaria transmission via blood transfusions or organ transplants becomes more prominent, particularly when screening protocols are inadequate. Congenital transmission, though less common, poses significant risks to infants born to infected mothers and can lead to severe complications if undiagnosed or untreated [11]. Additionally, shared needles or improper sterilization in healthcare settings can serve as a pathway for malaria transmission. These non-vector modes are particularly relevant in healthcare settings and regions where mosquito-borne transmission has been controlled but malaria persists due to lapses in healthcare protocols [12].

Despite their importance, non-vector transmission pathways are often underrepresented in mathematical models of malaria. Most existing models focus exclusively on mosquito-borne transmission, which creates gaps in understanding malaria dynamics, particularly in controlled environments where healthcare-associated transmission is more likely [13, 14]. Recent studies highlight the limitations of current models that focus on relapse mechanisms and asymptomatic carriers without incorporating the non-vector pathways that can sustain disease transmission [14, 15]. This oversight underscores the necessity of integrating non-vector transmission routes into existing frameworks to provide a more accurate representation of malaria dynamics.

To address these gaps, this study develops an expanded SEIR-based mathematical model that incorporates both vector and non-vector transmission pathways. Thus, this study introduces a novel malaria transmission model that uniquely integrates both vector-borne and non-vector transmission pathways within a modified SEIR framework. Unlike traditional models, which largely emphasize mosquito exposure, our approach incorporates vaccination efficacy, human-to-human transmission risks in healthcare settings, and the impact of blood transfusions. This refined model provides a more comprehensive and realistic simulation of malaria transmission dynamics, allowing for improved intervention strategies.

The human population is categorized into compartments for susceptible, vaccinated, exposed (via both vector and non-vector pathways), infectious, treated, and recovered individuals, while mosquitoes are classified into susceptible, exposed, and infectious populations. This model accounts for key factors such as vaccination efficacy, immunity loss, and progression rates from exposure to infection. By incorporating non-vector transmission pathways, the study aims to enhance the understanding of malaria transmission dynamics in diverse contexts.

The primary objectives of this study are to:

- Formulate a modified SEIR-based mathematical model that integrates both mosquito-borne and non-vector transmission routes, such as blood transfusions, congenital transmission, and organ transplants.
- Analyze the stability of the model's equilibria, including disease-free equilibrium state, to determine the conditions under which malaria can be controlled or eradicated.
- Investigate how incorporating non-vector transmission routes affects overall disease dynamics and evaluate the contributions of different transmission pathways to the disease burden.
- Generate insights and recommendations for public health policies and practices based on the model's findings.

By addressing the limitations of traditional vector-focused models, this study contributes to a more holistic approach to malaria management. The findings aim to guide policymakers in designing integrated control strategies that target both vector and non-vector transmission

routes, ultimately advancing efforts toward the global goal of malaria eradication.

Methods

To address the limitations of traditional malaria transmission models and provide a more comprehensive understanding of malaria dynamics, this study employs an advanced mathematical framework that incorporates both vector-borne and non-vector transmission routes. This section details the methodology used to develop, analyze, and validate this enhanced SEIR-based model.

Mathematical model formulation

The research work builds upon the SEIR model, which traditionally includes Susceptible (S), Exposed (E) and Infectious (I) compartments [7] for both human and mosquito populations and additional Recovered (R) compartment for human population. This model is expanded to include additional compartments for the human population: vaccinated individuals and non-vector exposed individuals, to account for non-vector transmission pathways in addition to the vector exposed individuals.

This model is formulated based on the following assumptions:

- The population is considered homogeneous in terms of susceptibility and exposure to malaria, meaning every individual has the same probability of being exposed to *Plasmodium* parasites and developing malaria [16].
- The rate at which malaria is transmitted from mosquitoes to humans remains constant over time. This implies that environmental and seasonal variations are not accounted for in the model [7].
- The distribution of malaria vectors (e.g., *Anopheles* mosquitoes) is uniform across the study area. This assumes that mosquito populations are evenly spread, which might not account for spatial heterogeneity [17].
- Birth and death rates in the population are fixed and do not vary with the prevalence of malaria. This means that demographic changes are not explicitly modeled [18].
- There is no migration or movement of individuals between areas with different malaria transmission rates. This simplifies the model by not considering the impact of human mobility on disease spread [2].
- The progression of malaria within an infected individual follows a fixed pattern, with a defined time from infection to the appearance of symptoms, treatment, and eventual recovery or death [19].
- The density of malaria vectors remains constant over time. This assumption ignores fluctuations in mosquito populations due to seasonal changes or interventions [20].
- Resources for malaria treatment (such as diagnostic tools and medical treatment) are evenly distributed across the population. This means that variations in access to healthcare services are not considered [21].
- Despite effective treatment, recovered individuals remain susceptible to reinfection if exposed to the parasite again. This is crucial in high-transmission settings where malaria recurs frequently (endemic areas) even after successful treatment [22].
- There is no vaccination for the human population that is free from malaria; vaccination is only present in the population where malaria is endemic [15].

Malaria model description

The malaria model formulated herein is subdivided into ten compartments of human and mosquito (vector) populations put together: Malaria Susceptible Human $S_H(t)$, Malaria Vaccinated Human $V_H(t)$, Malaria vector Exposed Human $E_{H1}(t)$, Malaria non-vector Exposed Human $E_{H2}(t)$, Malaria Infectious Human $I_H(t)$, Malaria treated Human $T_H(t)$, Malaria Recovered Human $R_H(t)$, Malaria Susceptible Mosquito $S_M(t)$, Malaria Exposed Mosquito $E_M(t)$ and Malaria Infectious Mosquito $I_M(t)$ Classes. Thus, the total population is given as;

$$N_{HM}(t) = N_H(t) + N_M(t)$$

where;

$$N_H(t) = S_H(t) + V_H(t) + E_{H1}(t) + E_{H2}(t) + I_H(t) + T_H(t) + R_H(t)$$

and

$$N_M(t) = S_M(t) + E_M(t) + I_M(t)$$

The Malaria susceptible human population class $S_H(t)$ is created by the birth rate $\pi(1-k)$ through with πk as the fraction of π that are already vaccinated, the population increases by the Malaria Vaccinated human loss of immunity rate θ, the Malaria recovered human immunity loss rate γ, the Malaria susceptible population reduces by having active contact rate with infectious vector β_2, by having active contact rate with infectious non-vector ways α_2 and also by natural death rate μ_1. The Malaria Vaccinated human class $V_H(t)$ is created through vaccinated π at the rate $k\pi$ with k as the fraction of π that are Malaria vaccinated, the Malaria vaccinated human population reduces by immunity loss rate θ, by having active contact rate with infectious vector β_1, by having active contact rate with infectious non-vector ways α_1 and also by natural death rate μ_1.. These people move up to Malaria vector exposed human class $E_{H1}(t)$ and Malaria

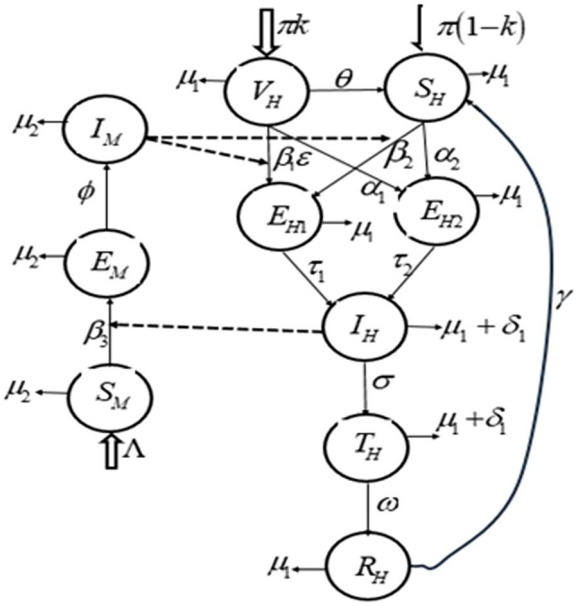

Fig. 1 Malaria model schematic diagram

Table 1 Malaria model variables description

Variables	Description
S_H	Malaria Susceptible human population
V_H	Malaria Vaccinated human population
E_{H1}	Mosquitoes (Vectors) Malaria Exposed human population
E_{H2}	Non – Mosquitoes (Non-vectors) Malaria Exposed human population
I_H	Malaria Infectious human population
T_H	Malaria Treated human population
R_H	Malaria Recovered human population
S_M	Malaria Susceptible Mosquitoes population
E_M	Malaria Exposed Mosquitoes population
I_M	Malaria Infectious Mosquitoes population

non-vector exposed human class $E_{H2}(t)$ when a Malaria exposed person in $E_{H1}(t)$ and $E_{H2}(t)$ exhibits clinical symptoms, they are moved into the Malaria infectious human class $I_H(t)$ at the rate τ_1 and τ_2 respectively, which causes both exposed classes to decrease while they also decrease by natural death rate μ_1. Some of those moved into the Malaria infectious human class $I_H(t)$ are moved into the Malaria treated human class $T_H(t)$ at the rate σ, when an infectious person in $I_H(t)$ recovers, they are moved into the Malaria recovered human class $R_H(t)$ at the rate ω which causes both $I_H(t)$ and $T_H(t)$ classes to decrease while they can also decrease by natural death rate μ_1 and disease related death at the rate δ_1. The Recovered human class $R_H(t)$ reduces by losing immunity and relapsing at the rate γ and natural death rate μ_1. The Malaria susceptible mosquito (vector) population class $S_M(t)$ is created by the birth rate Λ and reduces by having active contact at the rate β_3 and also by natural death rate μ_2. These mosquitoes move up to Malaria exposed mosquito class $E_M(t)$ when exposed mosquitoes becomes infectious, they are moved into the malaria infectious mosquitoes class $I_M(t)$ and they can die natural death at the rate μ_2.Where those in malaria infectious mosquito class $I_M(t)$ can die natural death at the rate μ_2.

The model flow diagram is presented as Fig. 1 below;

With the following terms defined as follows;

$$\beta_1 = \eta_V I_M,\ \beta_2 = \eta_S I_M,\ \alpha_1 = \xi_V I_H,\ \alpha_2 = \xi_S I_H \text{ and } \beta_3 = \rho I_H \tag{1}$$

The variable and parameter descriptions are presented in Tables 1 and 2 respectively.

The malaria model equations

Based on the flow diagram in Fig. 1, the description of the malaria dynamics is depicted by the following set of equations in Eq. (2) below:

$$\left.\begin{aligned}
(1)\ \frac{dS_H}{dt} &= \pi(1-k) + \theta V_H + \gamma R_H - (\mu_1 + \beta_2 + \alpha_2)S_H \\
(2)\ \frac{dV_H}{dt} &= \pi k - (\mu_1 + \theta + \beta_1\varepsilon + \alpha_1)V_H \\
(3)\ \frac{dE_{H1}}{dt} &= \beta_2 S_H + \beta_1\varepsilon V_H - (\mu_1 + \tau_1)E_{H1} \\
(4)\ \frac{dE_{H2}}{dt} &= \alpha_2 S_H + \alpha_1 V_H - (\mu_1 + \tau_2)E_{H2} \\
(5)\ \frac{dI_H}{dt} &= \tau_1 E_{H1} + \tau_2 E_{H2} - (\mu_1 + \delta_1 + \sigma)I_H \\
(6)\ \frac{dT_H}{dt} &= \sigma I_H - (\mu_1 + \delta_1 + \omega)T_H \\
(7)\ \frac{dR_H}{dt} &= \omega T_H - (\mu_1 + \gamma)R_H \\
(8)\ \frac{dS_M}{dt} &= \Lambda - (\mu_2 + \beta_3)S_M \\
(9)\ \frac{dE_M}{dt} &= \beta_3 S_M - (\mu_2 + \phi)E_M \\
(10)\ \frac{dI_M}{dt} &= \phi E_M - \mu_2 I_M
\end{aligned}\right\} \tag{2}$$

With Initial Condition:

$$\left.\begin{aligned}
&S_{H0} \geq 0,\ V_{H0} \geq 0, E_{H10} \geq 0, E_{H20} \geq 0,\ I_{H0} \geq 0, \\
&T_{H0} \geq 0,\ R_{H0} \geq 0,\ S_{M0} \geq 0,\ E_{M0} \geq 0 \text{ and } I_{M0} \geq 0
\end{aligned}\right\} \tag{3}$$

Table 2 Malaria model parameters description

Parameters	Description
π	Human Population birth rate
k	Vaccination rate
μ_1	Human Population Natural death rate
θ	Rate of vaccine immunity loss due to vaccine failure
ε	Rate of Vaccine Efficacy
η_V	Effective contact rate of Human Vaccinated individuals with infected mosquitoes through bloodmeals
η_S	Effective contact rate of Human susceptible individuals with infected mosquitoes through bloodmeals
ξ_V	Effective contact rate of Human Vaccinated individuals with infected humans through other non-mosquitoes' ways (non-vector pathways) of malaria infectivity
ξ_S	Effective contact rate of Human susceptible individuals with infected human through other non-mosquitos' ways (non-vector pathways) of malaria infectivity
τ_1	Human Population Progression rate from exposed to infectious for mosquitos' malaria exposed individuals
τ_2	Human Population Progression rate from exposed to infectious for non-mosquitos' (non-vector pathways) malaria exposed individuals
δ_1	Human Population Malaria disease death rate
σ	Human Population progression rate from infected to treated
ω	Human Population progression rate from treated to recovered
γ	Human recovered Population rate of immunity loss
Λ	Mosquitoes Population birth rate
ρ	Effective contact rate of susceptible mosquitoes with infected humans through bloodmeals
ϕ	Mosquitoes Population Progression rate from exposed to infectious
μ_2	Mosquitoes Population Natural death rate

Analysis of the malaria model

This analysis subsection focuses on evaluating the dynamics of the malaria transmission model through mathematical analysis.

Invariant region

In analyzing the model, establishing an invariant region is critical in other to ensure that the model's solutions are biologically meaningful. Because an invariant region guarantees that the state variables remain within realistic bounds and do not exceed the total population size.

Theorem 1 *The closed region*

$$\Omega = \left\{ (S_H, V_H, E_{H1}, E_{H2}, I_H, T_H, R_H, S_M, E_M, I_M) \in R_+^{10} : N_H(t) \leq \frac{\pi}{\mu_1}, N_M(t) \leq \frac{\Lambda}{\mu_2} \right\}$$

is a positively invariant set and attract all positive solutions of the model (2).

Proof We proceed with the proof by showing that the total population in both the human and mosquito compartments remains bounded over time.

Considering the human population;

$$N_H(t) = S_H(t) + V_H(t) + E_{H1}(t) + E_{H2}(t) + I_H(t) + T_H(t) + R_H(t)$$

$$\frac{N_H(t)}{dt} = \frac{S_H(t)}{dt} + \frac{V_H(t)}{dt} + \frac{E_{H1}(t)}{dt} + \frac{E_{H2}(t)}{dt} + \frac{I_H(t)}{dt} + \frac{T_H(t)}{dt} + \frac{R_H(t)}{dt}$$

$$\frac{N_H(t)}{dt} = \pi - \mu_1 N_H - \delta_1 (I_H + T_H)$$

By standard comparison theorem [23] we see that;

$$\frac{N_H(t)}{dt} \leq \pi - \mu_1 N_H$$

By integrating factor, we have;

$$\frac{N_H(t)}{dt} \leq \frac{\pi}{\mu_1} + \left[N_H(0) - \frac{\pi}{\mu_1} e^{-\mu_1 t} \right]$$

So that in particular,

$$\text{If } N_H(0) \leq \frac{\pi}{\mu_1} \text{ then } N_H(t) \leq \frac{\pi}{\mu_1}$$

Which shows that;

$$N_H(t) \leq \frac{\pi}{\mu_1}$$

Thus, the total human population remains bounded as $t \to \infty$ and the solution stays within the region $S_H(t) + V_H(t) + E_{H1}(t) + E_{H2}(t) + I_H(t) + T_H(t) + R_H(t) \leq N_H$.

Similarly,

Considering the mosquito population;

$$N_M(t) = S_M(t) + E_M(t) + I_M(t)$$

$$\frac{N_M(t)}{dt} = \frac{S_M(t)}{dt} + \frac{E_M(t)}{dt} + \frac{I_M(t)}{dt}$$

$$\frac{N_M(t)}{dt} = \Lambda - \mu_2 N_M$$

By standard comparison theorem [23] we see that

$$\frac{N_M(t)}{dt} \leq \Lambda - \mu_2 N_M$$

By integrating factor, we have;

$$\frac{N_M(t)}{dt} \leq \frac{\Lambda}{\mu_2} + \left[N_M(0) - \frac{\Lambda}{\mu_2} e^{-\mu_2 t}\right]$$

Which shows that

$$N_M(t) \leq \frac{\Lambda}{\mu_2}$$

Thus, the total mosquito population remains bounded as t→∞ and the solution stays within the region

$$S_M(t) + E_M(t) + I_M(t) \leq N_M.$$

Therefore, Ω is positively invariant and an attractor. So that no solution path leaves through any boundary of Ω. Thus, the set Ω will have solutions that are positive for all times. This means that the model (1) is epidemiologically well posed and biologically meaningful in the region Ω.

Malaria model disease free equilibrium (E^t)

Disease Free Equilibrium (DFE) of the model refers to a state where no individuals are infected with the malaria parasite in a given population, and the disease is absent from the population. It is a critical concept in mathematical epidemiology for understanding whether an infection will die out or persist in the long term. The malaria model DFE point is obtained by setting the number of infected individuals to zero.

Using the Malaria model system (2), at equilibrium or steady state the right-hand side of the equation is set to zero. Thus, at equilibrium Eq. (2) is given as;

$$\left.\begin{aligned}
&(1)\ \pi(1-k) + \theta V_H + \gamma R_H - (\mu_1 + \beta_2 + \alpha_2) S_H = 0\\
&(2)\ \pi k - (\mu_1 + \theta + \beta_1 \varepsilon + \alpha_1) V_H = 0\\
&(3)\ \beta_2 S_H + \beta_1 \varepsilon V_H - (\mu_1 + \tau_1) E_{H1} = 0\\
&(4)\ \alpha_2 S_H + \alpha_1 V_H - (\mu_1 + \tau_2) E_{H2} = 0\\
&(5)\ \tau_1 E_{H1} + \tau_2 E_{H2} - (\mu_1 + \delta_1 + \sigma) I_H = 0\\
&(6)\ \sigma I_H - (\mu_1 + \delta_1 + \omega) T_H = 0\\
&(7)\ \omega T_H - (\mu_1 + \gamma) R_H = 0\\
&(8)\ \Lambda - (\mu_2 + \beta_3) S_M = 0\\
&(9)\ \beta_3 S_M - (\mu_2 + \phi) E_M = 0\\
&(10)\ \phi E_M - \mu_2 I_M = 0
\end{aligned}\right\} \quad (4)$$

The malaria disease classes for human and mosquito populations are defined as $E_{H1}, E_{H2}, I_H, T_H, R_H, E_M, I_M$ and in the absence of malaria disease $E_{H1} = E_{H2} = I_H = T_H = R_H = E_M = I_M = 0$.

With the assumption that in the absence of malaria in the population there will be no vaccine. We have, $V_H = 0$ also at malaria disease free equilibrium.

Adding Eqs. (1) − (7) in (3) above we have

$$\pi - \mu_1 N_H - \delta_1 (I_H + T_H) = 0$$
$$Where\ N_H = S_H + E_{H1} + E_{H2} + I_H + T_H + R_H$$
$$And\ V_H = E_{H1} = E_{H2} = I_H = T_H = R_H = 0$$

Thus,

$$\pi - \mu_1 S_H = 0$$

so that

$$\pi - \mu_1 S_H^t = 0 \text{ where } S_H^t = S_H \ at\ malaria\ disease\ free\ equilibrium\ state$$

$$\Rightarrow S_H^t = \frac{\pi}{\mu_1}$$

Adding Eqs. (8) − (10) in (3) above we have

$$\Lambda - \mu_2 N_M = 0$$
$$\text{Where } N_M = S_M + E_M + I_M$$
$$\text{And } E_M = I_M = 0$$

Thus,

$$\Lambda - \mu_2 S_M = 0$$

So that

$$\Lambda - \mu_2 S_M^t = 0 \text{ Where } S_M^t = S_M \ at\ malaria\ disease\ free\ equilibrium\ state$$

$$\Rightarrow S_M^t = \frac{\Lambda}{\mu_2}$$

From the above, the malaria disease free equilibrium point of the malaria model (2) is given as;

$$E^t = \{S_H^t, E_{H1}^t, E_{H1}^t, I_H^t, T_H^t, R_H^t, S_M^t, E_M^t, I_M^t\} = \left\{\frac{\pi}{\mu_1}, 0, 0, 0, 0, 0, 0, \frac{\Lambda}{\mu_2}, 0, 0\right\}$$

Therefore, E^t represents the equilibrium state in which there is no malaria infection (absence of malaria) in the population.

Malaria model basic reproduction number (R_0)

The basic reproduction number denoted by R_0 is a parameter which its value is used to determine how long a disease like malaria will prevail in a particular population. If $R_0 < 1$, it implies that an infected individual produces in average less than one infected person in a population and by that it means that with time the disease will die out of

the population. But if $R_0 > 1$, it implies that an infected individual produces more than one infected person in a population and by that it means that with time surely the disease will not die out of the population. Thus, for any disease such as malaria to die out of any population R_0 must be less than one (unity). The method used to calculate this is called the next generation method which was used in [24]. Applying the next generation method to our malaria model (2) considering the infective classes $E_{H1}, E_{H2}, I_H, T_H, E_M, I_M$ we have F_i *and* V_i are defined as follows;

$$F_i = \begin{bmatrix} \eta_S I_M S_H + \eta_V I_M \varepsilon V_H \\ \xi_S I_H S_H + \xi_V I_H V_H \\ 0 \\ 0 \\ \rho I_H S_M \\ 0 \end{bmatrix} \text{ and } V_i = \begin{bmatrix} (\mu_1+\tau_1)E_{H1} \\ (\mu_1+\tau_2)E_{H2} \\ (\mu_1+\delta_1+\sigma)I_H - \tau_1 E_{H1} - \tau_2 E_{H2} \\ (\mu_1+\delta_1+\omega)T_H - \sigma I_H \\ (\mu_2+\phi)E_M \\ \mu_2 I_M - \phi E_M \end{bmatrix}$$

Linearizing the matrix, we obtained the Jacobian Matrix of the partial derivatives of F_i with respect to $E_{H1}, E_{H2}, I_H, T_H, E_M, I_M$ at disease free equilibrium point E^t given as;

$$F = \begin{bmatrix} 0&0&0&0&0&a_1 \\ 0&0&a_2&0&0&0 \\ 0&0&0&0&0&0 \\ 0&0&0&0&0&0 \\ 0&0&a_3&0&0&0 \\ 0&0&0&0&0&0 \end{bmatrix} \quad \text{and} \quad V = \begin{bmatrix} a&0&0&0&0&0 \\ 0&b&0&0&0&0 \\ -g&-h&c&0&0&0 \\ 0&0&-n&d&0&0 \\ 0&0&0&0&e&0 \\ 0&0&0&0&-m&f \end{bmatrix}$$

Malaria model endemic equilibrium (E^s)

The Endemic Equilibrium (EE) of the malaria model refers to the state where the malaria disease persists in the population at a constant level, without either increasing or decreasing over time. This equilibrium occurs when the basic reproduction number is greater than unity, meaning that each infected individual, on average, causes more than one new infection. We obtain the endemic equilibrium point by setting the time derivatives of the model compartments to zero as in Eq. (3) and solve simultaneously to obtain the endemic equilibrium point as;

$$E^s = \{S_H^s, V_H^s, E_{H1}^s, E_{H1}^s, I_H^s, T_H^s, R_H^s, S_M^s, E_M^s, I_M^s\} \neq \{0,0,0,0,0,0,0,0,0,0\}$$

where,

$a_1 = \eta_S S_H^t, a_2 = \xi_S S_H^t, a_3 = \rho S_M^t, a = (\mu_1+\tau_1), b = (\mu_1+\tau_2), c = (\mu_1+\delta_1+\sigma), d = (\mu_1+\delta_1+\omega),$
$e = (\mu_2+\phi), f = \mu_2, g = \tau_1, h = \tau_2, m = \phi, n = \sigma.$

Using MATLAB Software, we computed V^{-1}, $F * V^{-1}$ and obtained;

$$V^{-1} = \begin{bmatrix} \frac{1}{a}&0&0&0&0&0 \\ 0&\frac{1}{b}&0&0&0&0 \\ \frac{g}{ac}&\frac{h}{bc}&\frac{1}{c}&0&0&0 \\ \frac{ng}{dca}&\frac{nh}{dcb}&\frac{n}{dc}&\frac{1}{d}&0&0 \\ 0&0&0&0&\frac{1}{e}&0 \\ 0&0&0&0&\frac{m}{ef}&\frac{1}{f} \end{bmatrix} \quad \text{and} \quad FV^{-1} = \begin{bmatrix} 0&0&0&0&\frac{a_1 m}{ef}&\frac{a_1}{f} \\ \frac{a_2 g}{ac}&\frac{a_2 h}{bc}&\frac{a_2}{c}&0&0&0 \\ 0&0&0&0&0&0 \\ 0&0&0&0&0&0 \\ \frac{a_3 g}{ac}&\frac{a_3 h}{bc}&\frac{a_3}{c}&0&0&0 \\ 0&0&0&0&0&0 \end{bmatrix}$$

We also obtained the eigenvalue of FV^{-1} as follows;

$$eig\left(FV^{-1}\right) = \begin{bmatrix} 0 \\ 0 \\ 0 \\ 0 \\ \frac{efaha_2 - \sqrt{(e^2f^2a^2h^2a_2^2 + 4acb^2efa_1ma_3g)}}{2abcef} \\ \frac{efaha_2 + \sqrt{(e^2f^2a^2h^2a_2^2 + 4acb^2efa_1ma_3g)}}{2abcef} \end{bmatrix}$$

where the eigenvalues are as follows;

$$\lambda_1 = 0, \lambda_2 = 0, \lambda_3 = 0, \lambda_4 = 0, \lambda_5 = \frac{efaha_2 - \sqrt{(e^2f^2a^2h^2a_2^2 + 4acb^2efa_1ma_3g)}}{2abcef} \text{ and}$$
$$\lambda_6 = \frac{efaha_2 + \sqrt{(e^2f^2a^2h^2a_2^2 + 4acb^2efa_1ma_3g)}}{2abcef}$$

$R_0 = \rho\left(FV^{-1}\right)$ is given as the largest eigenvalue of FV^{-1} which in this case is λ_6.

Therefore,

$$R_0 = \frac{efaha_2 + \sqrt{(e^2f^2a^2h^2a_2^2 + 4acb^2efa_1ma_3g)}}{2abcef}$$

Simplifying we have,

$$R_0 = \frac{1}{2}\left[\frac{a_2h}{bc} + \sqrt{\left(\frac{a_2h}{bc}\right)^2 + 4\left(\frac{a_1ma_3g}{acef}\right)}\right] \text{ and } R_0 = \frac{1}{2}\left[R_{01} + \sqrt{R_{01}^2 + 4R_{02}R_{03}}\right]$$

where

$$R_{01} = \frac{a_2h}{bc} = \frac{\xi_S\pi\tau_2}{\mu_1(\mu_1+\tau_2)(\mu_1+\delta_1+\sigma)},\ R_{02} = \frac{a_1g}{ac} = \frac{\eta_S\pi\tau_1}{\mu_1(\mu_1+\tau_1)(\mu_1+\delta_1+\sigma)} \text{ and } R_{03} = \frac{a_3m}{ef} = \frac{\rho\Lambda}{\mu_2^2(\mu_2+\phi)}$$

With;

$$T_H^s = \frac{\sigma I_H^s}{(\mu_1+\delta_1+\omega)}, R_H^s = \frac{\omega\sigma I_H^s}{(\mu_1+\gamma)(\mu_1+\delta_1+\omega)}, V_H^s = \frac{\pi k}{(\mu_1+\theta+\beta_1\varepsilon+\alpha_1)} = B, S_H^s = \frac{H+M+Z I_H^s}{A},$$

where;

$$H = \pi(\mu_1+\gamma)(\mu_1+\delta_1+\omega)(\mu_1+\theta+\beta_1\varepsilon+\alpha_1)(1-k), M = \theta(\mu_1+\gamma)(\mu_1+\delta_1+\omega), Z = \gamma\omega\sigma$$

and $A = (\mu_1+\beta_2+\alpha_2)(\mu_1+\gamma)(\mu_1+\delta_1+\omega)(\mu_1+\theta+\beta_1\varepsilon+\alpha_1)$

$$E_{H1}^s = \frac{\beta_2(H+M+Z I_H^s)+\beta_1\varepsilon BA}{A(\mu_1+\tau_1)}, E_{H2}^s = \frac{\alpha_2(H+M+Z I_H^s)+\alpha_1 BA}{A(\mu_1+\tau_2)}, I_H^s = \frac{D}{C - Z(\tau_1\beta_2+\tau_2\alpha_2)},$$

where;

$D = (H+M)(\tau_1\beta_2+\tau_2\alpha_2)+AB(\tau_1\beta_1\varepsilon+\tau_2\alpha_1)$ *and* $C = A(\mu_1+\tau_1)(\mu_1+\tau_2)(\mu_1+\delta_1+\sigma)$.

$$S_M^s = \frac{\mu_2(\mu_2+\phi)I_M^s}{\phi\beta_3}, E_M^s = \frac{\mu_2 I_M^s}{\phi} \text{ and } I_M^s = \frac{\phi\beta_3\Lambda}{\mu_2(\mu_2+\beta_3)(\mu_2+\phi)}.$$

Seeing that the Susceptible, Exposed, Treated and Recovered human populations depends on the infectious human population and the Susceptible and Exposed mosquito population depends on the infectious mosquito population while both human and mosquito infectious populations depends on their force of infection. This implies that at this equilibrium point there will always be malaria in the population at all time.

Theorem 2 *The malaria DFE point* (E^t) *of the malaria model Eq.* (2) *is Locally Asymptotically Stable* (*LAS*) *whenever* $R_0 < 1$ *and unstable when otherwise.*

Proof Applying eigenvalue analysis and the Routh-Hurwitz criterion [25] we linearize the model system of differential Eqs. (2) around its DFE and the resulting Jacobian matrix is given as;

$$J_{10} = \begin{bmatrix} -\mu_1 & 0 & 0 & 0 & -a_2 & 0 & \gamma & 0 & 0 & -a_1 \\ 0 & -\mu_1 & 0 & 0 & 0 & 0 & 0 & 0 & 0 & 0 \\ 0 & 0 & -a & 0 & 0 & 0 & 0 & 0 & 0 & 0 \\ 0 & 0 & 0 & -b & a_2 & 0 & 0 & 0 & 0 & 0 \\ 0 & 0 & g & h & -c & 0 & 0 & 0 & 0 & 0 \\ 0 & 0 & 0 & 0 & n & -d & 0 & 0 & 0 & 0 \\ 0 & 0 & 0 & 0 & 0 & p & -q & 0 & 0 & 0 \\ 0 & 0 & 0 & 0 & -a_3 & 0 & 0 & -\mu_2 & 0 & 0 \\ 0 & 0 & 0 & 0 & a_3 & 0 & 0 & 0 & -e & 0 \\ 0 & 0 & 0 & 0 & 0 & 0 & 0 & 0 & m & -f \end{bmatrix}$$

where

$a_1 = \eta_S S_H^t, a_2 = \xi_S S_H^t, a_3 = \rho S_M^t, a = (\mu_1+\tau_1), b = (\mu_1+\tau_2), c = (\mu_1+\delta_1+\sigma), q = (\mu_1+\gamma),$
$d = (\mu_1+\delta_1+\omega), e = (\mu_2+\phi), f = \mu_2, g = \tau_1, p = \omega, h = \tau_2, n = \sigma, m = \phi.$

Local stability of the malaria model DFE (E^t)

Local stability analysis near the malaria model DFE (E^t) provides insight into the early stages of malaria transmission, where only a small number of infected individuals are introduced into a susceptible population. Analyzing the local stability of the DFE is crucial because it allows us to understand under what conditions a disease can invade or die out within a population.

The characteristic equation $|J_{10} - \lambda I_{10}|$ admits five (5) eigenvalues as

$$\lambda_1 = -\mu_1 < 0, \lambda_2 = -\mu_1 < 0, \lambda_3 = -\mu_2 < 0, \lambda_4 = -d < 0 \text{ and } \lambda_5 = -q < 0$$

With the remaining eigenvalues determined from the submatrix

$$J_5 = \begin{bmatrix} -a & 0 & 0 & 0 & a_1 \\ 0 & -b & a_2 & 0 & 0 \\ g & h & -c & 0 & 0 \\ 0 & 0 & a_3 & -e & 0 \\ 0 & 0 & 0 & m & -f \end{bmatrix}$$

Using MATLAB software, we obtained the characteristic polynomial of J_5as

$$F(\lambda) = A_0\lambda^5 + A_1\lambda^4 + A_2\lambda^3 + A_3\lambda^2 + A_4\lambda^1 + A_5\lambda^0$$

where;

$$A_0 = 1 > 0,\ A_1 = a + b + c + e + f > 0,$$

$$A_2 = ab + ac + ae + af + be + bf + ce + cf + ef + bc(1 - R_{01}) > 0 \ \textit{when}\ R_{01} < 1,$$

$$A_3 = abe + abf + ace + acf + aef + bef + cef + \big(abc + bce + bcf\big)(1 - R_{01}) > 0 \ \textit{when}\ R_{01} < 1,$$

$$A_4 = aef\big(b + c(1 - R_{02}R_{03}) + bc\big(ae + af + ef\big)(1 - R_{01})\big) > 0 \ \textit{when}\ R_{01} < 1 \ \textit{and}\ R_{02}R_{03} < 1,$$

$$A_5 = abcef\,(1 - (R_{01} + R_{02}R_{03})) > 0 \ \textit{when}\ R_{01} < 1 \ \textit{and}\ R_{02}R_{03} < 1.$$

Thus,

$A_0 > 0$ *and* $A_1 > 0$ *with*

$A_2 > 0, A_3 > 0, A_4 > 0$ *and* $A_5 > 0$ *whenever* $R_0 < 1$.

According to Routh-Hurwitz criteria [25], it can be seen that the characteristic polynomial $F(\lambda)$ has all negative real roots whenever $R_0 < 1$. Therefore, the DFE point (E^t) is locally asymptotically stable whenever $R_0 < 1$. But unstable when otherwise. Epidemiologically, this means that the malaria transmission in the population can be controlled when $R_0 < 1$ and uncontrollable when otherwise.

Results

In this section, we perform the malaria model numerical analysis presenting the key findings and interpreting their significance within the broader context of malaria transmission modeling. This section provides summary of the result derived from the model numerical simulations. The parameter values for the numerical analysis were sourced and recorded in Table 3 with their sources referenced.

Using MATLAB Software, the numerical simulation of the malaria model was performed with the following initial values;

$$S_H = 800,\ V_H = 50, E_{H1} = 30, E_{H2} = 20,\ I_H = 15,$$
$$T_H = 10,\ R_H = 5,\ S_M = 5,\ E_M = 5\,\textit{and}\ \ I_M = 5.$$

The results obtained are as follows;

The dashed curve shows a declining trend in the susceptible human population as more individuals get exposed to malaria. The solid green curve represents individuals already exposed to malaria through mosquito bites but not yet infectious known as the vector exposed human population. The red curve accounts for those exposed to malaria through non-vector means known as the non-vector exposed human population. The overall graph trend shows an initial rise in the exposed populations while the susceptible population decreases due to new infections Figs. 2 and 3.

The blue dashed curve represents individuals that are receiving vaccination, which may increase initially before stabilizing. The red curve shows a rapid increase in the infections human population, reaching a peak before declining, likely due to recovery, treatment, or immunity. The interaction between these two groups highlights how vaccination contributes to slowing down of malaria infection spread but does not immediately eradicate the disease.

These results indicate that vaccination significantly reduces susceptibility to malaria, with numerical simulations showing an approximate 43% reduction in the susceptible human population. This demonstrates the effectiveness of vaccination in reducing the overall disease burden, though it does not entirely eliminate the risk of transmission Fig. 4.

The blue dashed curve represents individuals that are receiving treatment, which initially increases as infections increase. The red curve shows the number of individuals who recover and develop immunity over time. The overall trend indicates that treatment leads to a steady increase in recovered individuals, contributing to the malaria disease control Fig. 5.

The blue dashed curve represents uninfected mosquitoes capable of transmitting malaria. The green curve shows mosquitoes that have acquired the malaria parasite but are not yet infectious. The red curve rises initially as more mosquitoes become infectious before declining, due to natural mortality or control interventions. The trend in infectious mosquitoes closely follows human infections, emphasizing the importance of vector control in the mitigation of malaria disease Fig. 6.

Table 3 Parameter values and their sources

Parameters	Value	References
π	0.012 per day (annual birth rate)	[26]
k	0.60—0.90 (estimate based on vaccination campaigns)	[27]
μ_1	0.0002 per day (India's average human mortality rate)	[28]
μ_2	0.1 per day (based on mosquito lifespan)	[28]
Λ	0.02 per day (estimate for malaria-endemic areas)	[26]
ε	0.3—0.5	[28, 29]
θ	0.1—0.2	[28, 29]
τ_1	0.05 per day (based on incubation period of 14 days)	[28]
τ_2	0.05 per day (same as vector-exposed)	[26]
σ	0.10 per day (estimate based on treatment coverage)	[26]
ω	0.05 per day	[28]
γ	0.01 per day (varies by region and immunity)	[27]
δ_1	0.002 per day	[28]
Φ	0.10 per day	[28]
η_V	0.001—0.005 per day	[30]
η_S	0.005—0.02 per day	[27]
ξ_V	0.0005—0.002 per day	[28]
ξ_S	0.001—0.003 per day	[26]
ρ	0.01—0.05 per mosquito	[28]

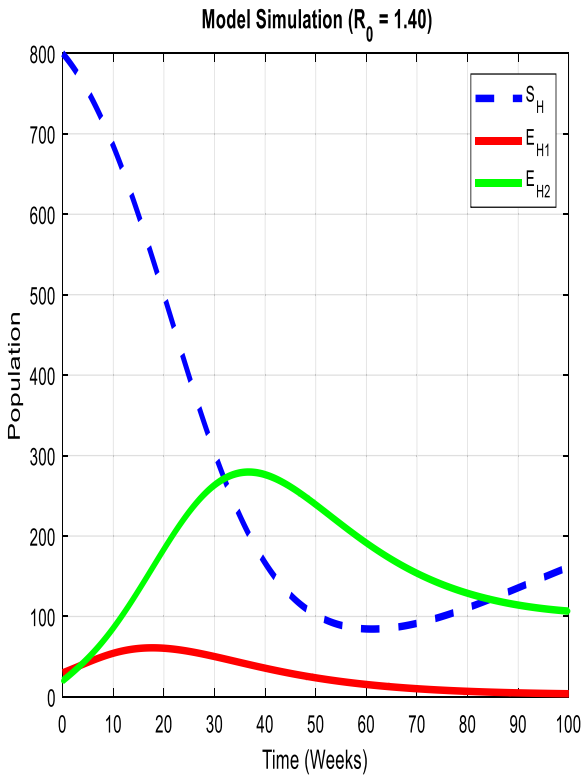

Fig. 2 Graph of susceptible, vector-exposed, and non-vector-exposed human populations

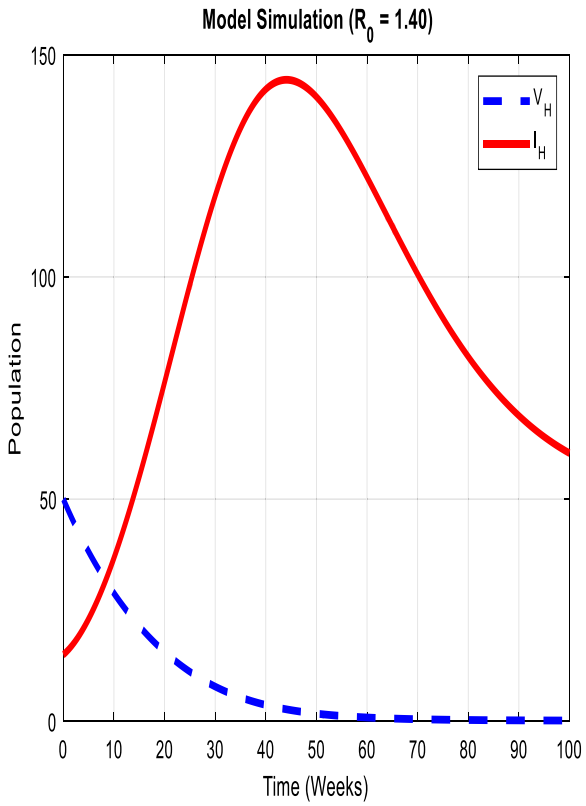

Fig. 3 Graph of vaccinated humans and infected humans populations

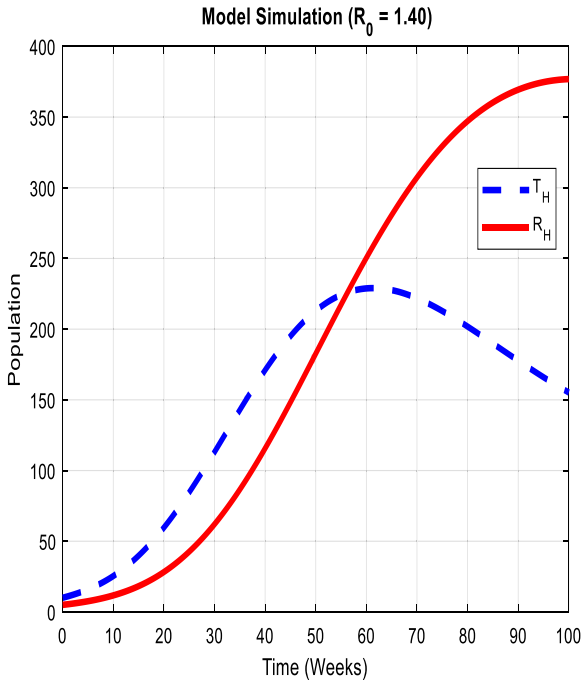

Fig. 4 Graph of treated humans and recovered humans populations

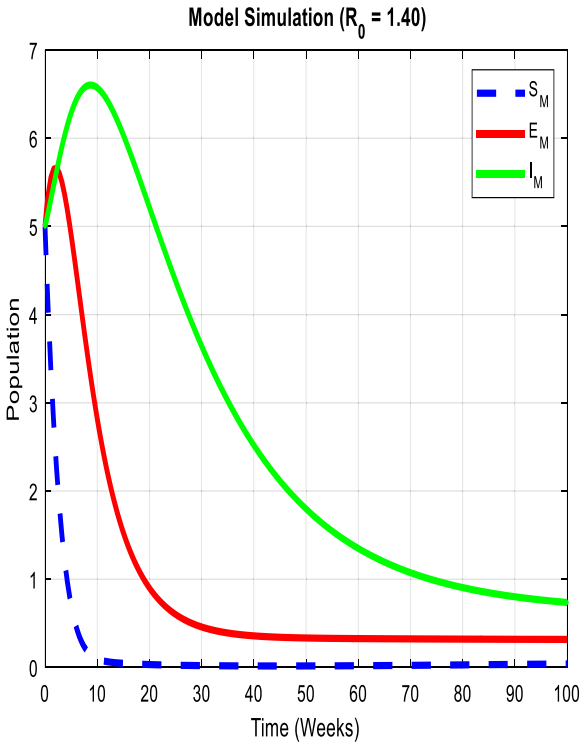

Fig. 5 Graph of susceptible, exposed, and infectious mosquito populations

This plot shows how the number of vector exposed humans changes over time for different values of ξ_S. The number of vector exposed individuals initially rises, peaks, and then declines as time progresses. Higher values of ξ_S result in a lower peak, while lower $\boldsymbol{\xi_S}$ results in higher peak. This suggests that when ξ_S is high, more infections occur directly between humans, meaning fewer susceptible individuals get exposed through mosquitoes. As a result, mosquitoes have fewer chances to acquire the pathogen from infected humans, leading to a smaller vector-exposed population. Lower ξ_S Means Greater Dependence on Vector Transmission. When human-to-human transmission ξ_S is low, the main infection route is mosquito-mediated transmission. This increases mosquito exposure to infected humans, leading to a higher vector-exposed population (since more mosquitoes are acquiring the infection) Fig. 7.

This plot represents the vector-exposed human population with varying effect of η_S. These are individuals who were bitten by an infected mosquito but are not yet infectious. The number of vector-exposed humans increases, peaks early, and then decline over time. Higher values of η_S lead to a higher exposure peak, indicating that higher mosquito -to-human exposure will increase the number of newly vector exposed individuals. The lowest η_S shows the lowest peak, indicating that lower mosquito-to-human exposure will lead to smaller number of newly vector exposed individuals Fig. 8.

This plot represents humans exposed to malaria through non-mosquito sources (e.g., congenital transmission or blood transfusion) over time. Higher values of ξ_S increases the peak exposure in non-vector transmission routes, suggesting that higher human-to-human exposure increases both mosquito and non-mosquito transmission routes. The smallest $\xi_S$has the lowest peak, showing that when human-to-human exposure is minimal, non-vector exposure reduces significantly Fig. 9.

This plot tracks the effect of varying η_S on non-vector-exposed individuals over time. Infections increase, peak, and then gradually decline for each varying value of η_S. Higher η_S values lower the infection peak, suggesting that as η_S increases, the peak of the non-vector exposed population decreases. This also shows that mosquito-borne transmission is becoming the dominant infection route, diverting individuals away from the non-vector exposed category Fig. 10.

This plot shows how the number of infectious human changes over time for different values of $\boldsymbol{\xi_S}$. The infectious human population initially rises, reaching a peak before gradually declining. Higher values of $\boldsymbol{\xi_S}$ lead to a higher peak and a prolonged infection period, suggesting that $\boldsymbol{\xi_S}$ plays a role in increasing the infection rate or transmission intensity. Lower values of $\boldsymbol{\xi_S}$ result in a

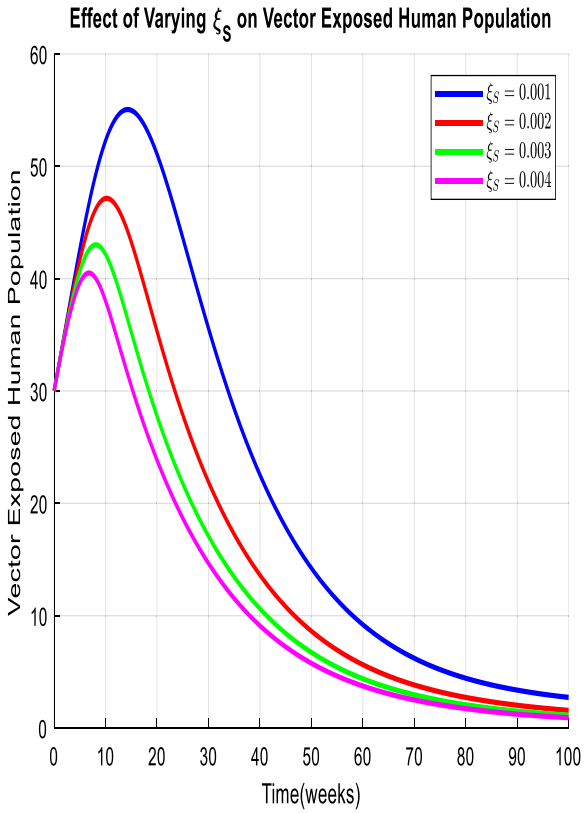

Fig. 6 Effect of Varying ξ_S on Vector Exposed Human Population

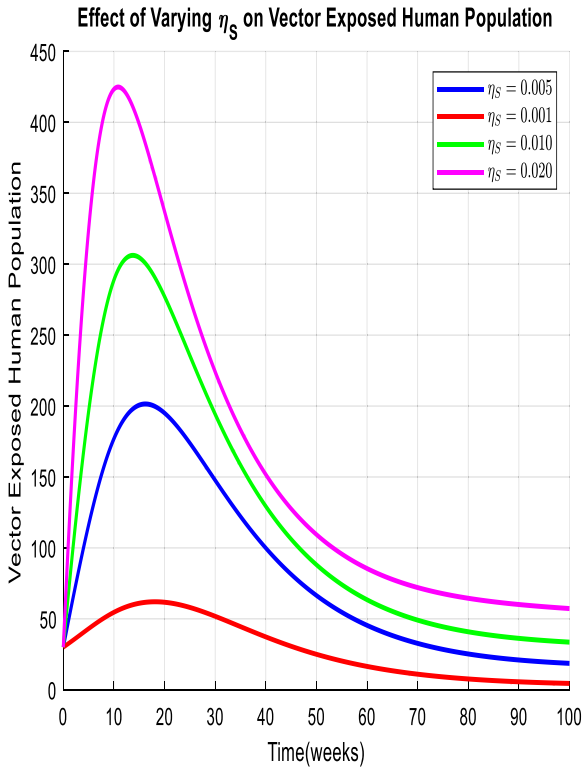

Fig. 7 Effect of Varying η_S on Vector Exposed Human Population

slower rise and a lower peak, indicating reduced transmission or progression to infection Fig. 11.

This plot illustrates how changes in $\boldsymbol{\eta_S}$ impact the infectious human population over time. The number of infectious humans initially rises, peaks, and then declines. Higher values of $\boldsymbol{\eta_S}$ result in a higher peak and a faster decline, suggesting that increasing $\boldsymbol{\eta_S}$ increases infection levels. Lower values of $\boldsymbol{\eta_S}$ reduces the infectious period and lead to a lesser infection burden Fig. 12.

This plot shows how the infectious mosquito population evolves over time with different values of $\boldsymbol{\xi_S}$. The infectious mosquito population initially increases and then stabilizes. Higher $\boldsymbol{\xi_S}$ values lead to a greater initial rise, indicating a stronger impact of $\boldsymbol{\xi_S}$ on mosquito infection dynamics. This suggests that $\boldsymbol{\xi_S}$ influences the transmission cycle between mosquitoes and humans. The stabilization phase indicates a balance between new infections and natural mortality or recovery Fig. 13.

This plot examines the impact of varying $\boldsymbol{\eta_S}$ on the infectious mosquito population over time. Unlike the human infection case, the mosquito population shows a relatively uniform decline across all $\boldsymbol{\eta_S}$ values, with minimal differences between the curves. This suggests that $\boldsymbol{\eta_S}$ primarily affects human infection dynamics, with limited direct influence on the mosquito population. The observed decline indicates that infected mosquitoes are either dying or aging out of the infectious stage Fig. 14.

This plot shows how the number of treated humans changes over time for different values of $\boldsymbol{\xi_S}$. The treated population initially rises as more individuals receive treatment, reaching a peak before gradually declining. Higher values of $\boldsymbol{\xi_S}$ lead to an earlier and higher peak, suggesting that increasing $\boldsymbol{\xi_S}$ enhances the rate at which infected individuals seek or receive treatment. Lower values of $\boldsymbol{\xi_S}$ result in a slower rise and lower peak, indicating delayed or reduced treatment uptake Fig. 15.

This plot illustrates the effect of varying $\boldsymbol{\eta_S}$ on the treated human population over time. The treated population follows a similar trend to Fig. 17, with an initial rise followed by a gradual decline. Higher $\boldsymbol{\eta_S}$ values result in a lower peak and a faster decline, indicating that increasing $\boldsymbol{\eta_S}$ might lead to quicker recovery or reduced need for prolonged treatment. Lower values of $\boldsymbol{\eta_S}$ cause a sustained increase in the treated population, suggesting a longer duration of treatment dependency Fig. 16.

This plot shows the growth of the recovered human population over time for different values of $\boldsymbol{\xi_S}$. The number of recovered individuals increases steadily, with minor variations across different $\boldsymbol{\xi_S}$ values. Higher $\boldsymbol{\xi_S}$ values lead to a slightly faster accumulation of recovered

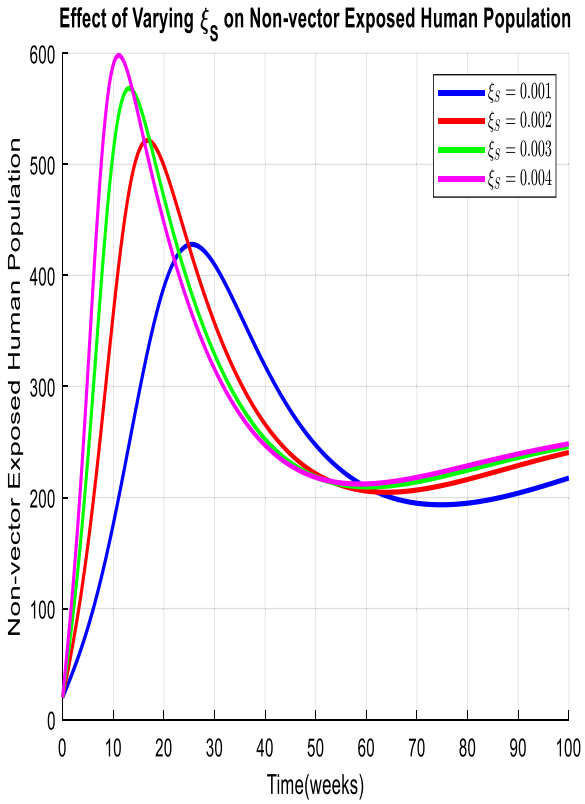

Fig. 8 Effect of Varying ξ_S on Non-Vector Exposed Human Population

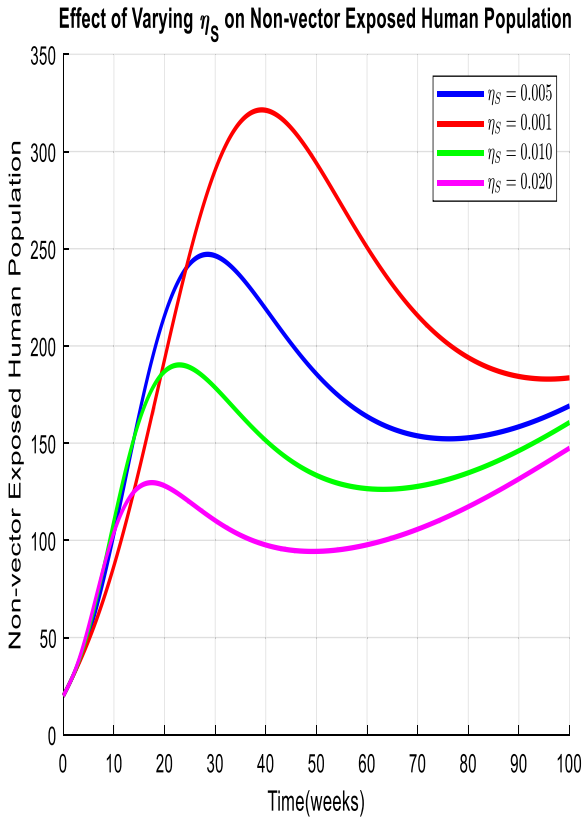

Fig. 9 Effect of Varying η_S on Non-Vector Exposed Human Population

individuals, indicating that increasing $\boldsymbol{\xi_S}$ enhances the transition from infection or treatment to recovery. However, the overall difference between the curves remains small, suggesting a more gradual and stable effect Fig. 17.

This plot examines how changes in $\boldsymbol{\eta_S}$ influence the recovered human population over time. Similar to Fig. 16, the recovered population steadily increases. Higher values of $\boldsymbol{\eta_S}$ lead to a slightly faster recovery rate, suggesting that $\boldsymbol{\eta_S}$ positively affects the transition from infection or treatment to full recovery. However, the differences between the curves remain minimal, indicating that while $\boldsymbol{\eta_S}$ influences recovery, its impact is more gradual.

Discussion

The findings from the model simulations presented in the results section provide valuable insights into the dynamics of malaria transmission and the effectiveness of control interventions. Specifically, the dynamics of both human and mosquito populations were analyzed, taking into account both vector-borne and non-vector transmission pathways.

Impact of vaccination on susceptibility

Impact of Vaccination on Susceptibility**:** The analysis of the susceptible human population and the vaccinated human population highlights the critical role of vaccination in reducing malaria susceptibility. The numerical results indicate a 43% reduction in malaria susceptibility among vaccinated individuals, confirming the protective effect of vaccination. However, the persistence of infectious individuals suggests that vaccination alone is insufficient for eradication and must be complemented by robust vector control and non-vector transmission interventions. The model shows that increasing vaccination coverage significantly reduces the number of susceptible individuals, which in turn helps limit the spread of malaria. However, the results also underscore the challenges in achieving complete vaccination coverage, especially in regions with logistical barriers or vaccine hesitancy. The results align with existing literature, which suggests that while vaccination can significantly reduce malaria transmission, it must be part of a broader, integrated strategy that includes other interventions like vector and non-vector control.

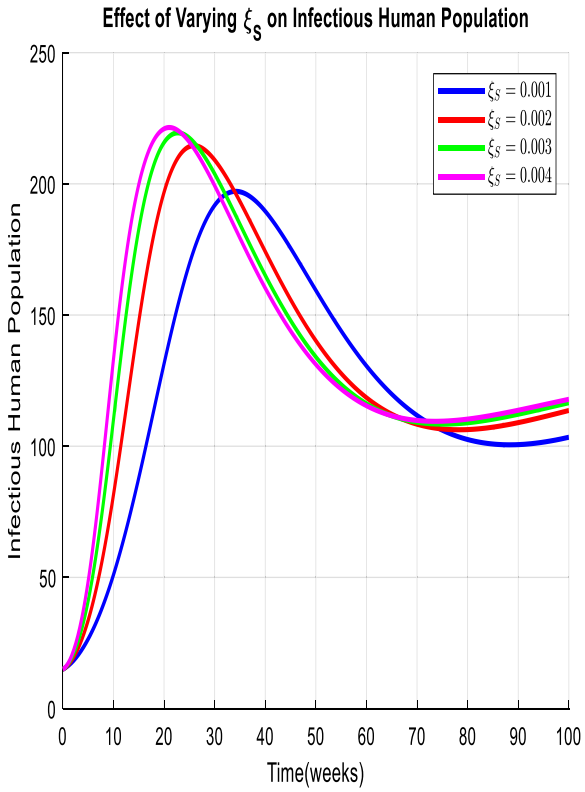

Fig. 10 Effect of Varying ξ_S on Infectious Human Population

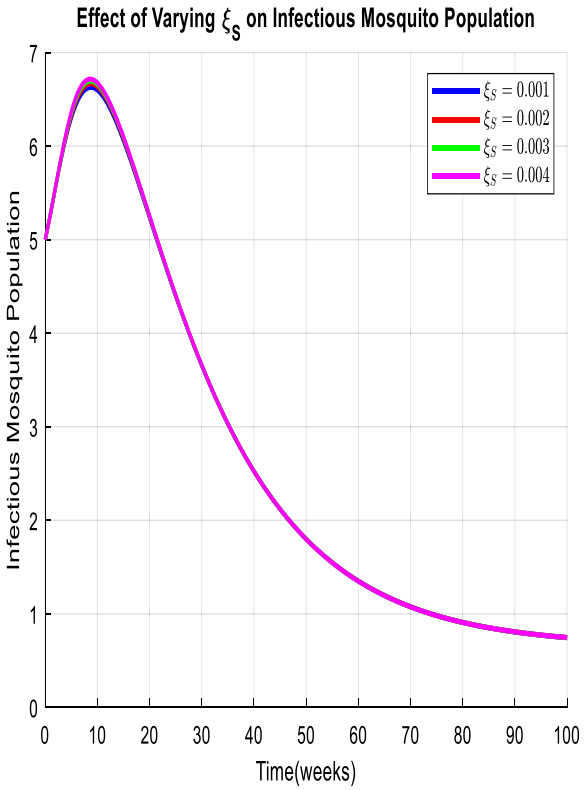

Fig. 12 Effect of Varying ξ_S on Infectious Mosquito Population

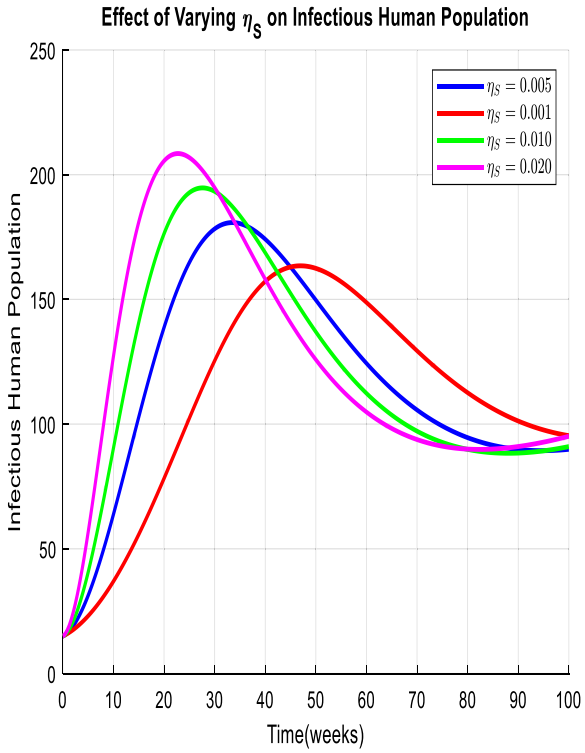

Fig. 11 Effect of Varying η_S on Infectious Human Population

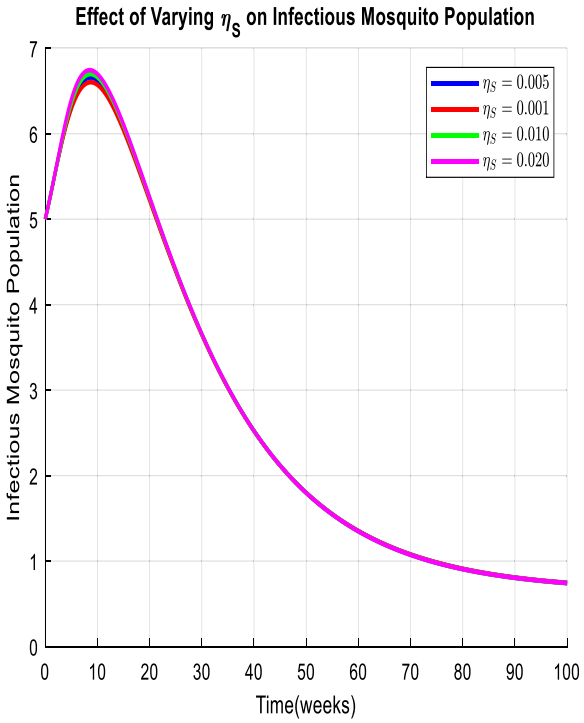

Fig. 13 Effect of Varying η_S on Infectious Mosquito Population

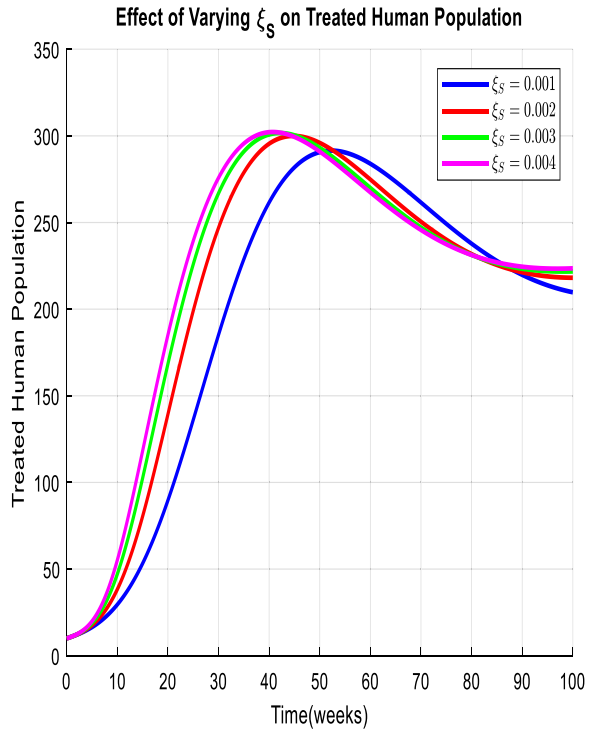

Fig. 14 Effect of Varying ξ_S on Treated Human Population

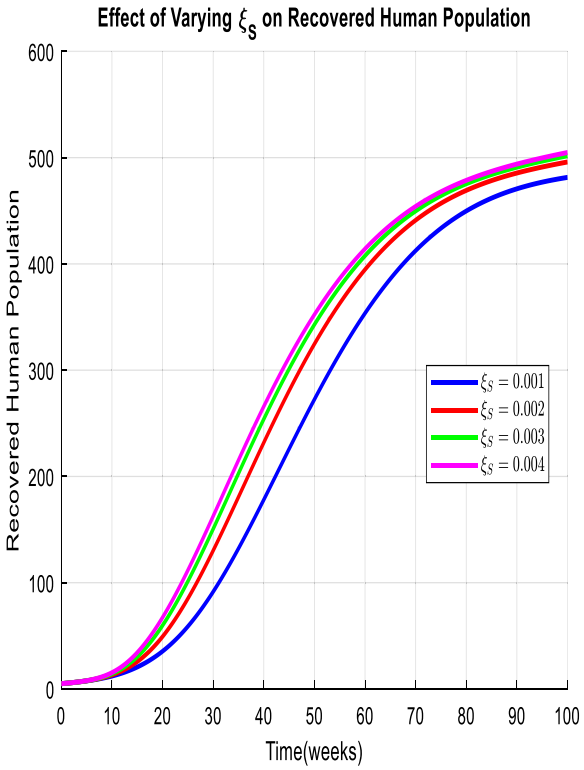

Fig. 16 Effect of Varying ξ_S on Recovered Human Population

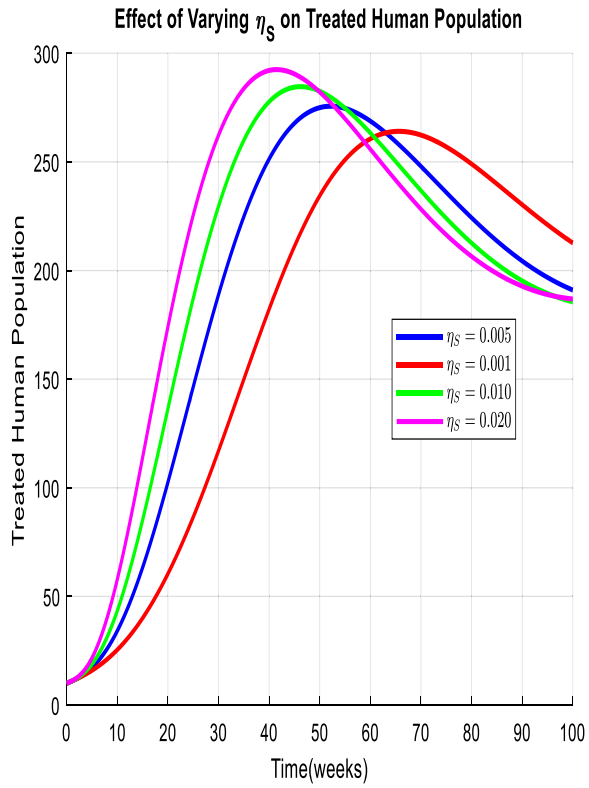

Fig. 15 Effect of Varying η_S on Treated Human Population

Vector and non-vector transmission dynamics

The dynamics of the vector-exposed human population and the non-vector exposed human population indicate that both mosquito-borne and non-mosquito pathways contribute to malaria transmission. The significant role of non-vector transmission, such as through blood transfusions or congenital transmission, highlights the limitations of focusing solely on vector control. While effective vector control can reduce mosquito exposure, non-vector transmission routes may sustain the disease in areas where mosquito populations are under control. This supports recent studies [9, 10] that emphasize the need for broader interventions that address both vector and non-vector transmission pathways.

Infectious human and mosquito populations

The infectious human population and infectious mosquito population demonstrate the ongoing risk of malaria transmission even when a large portion of the population has been vaccinated or treated. The persistence of an infectious pool in both humans and mosquitoes underscores the importance of rapid response interventions to reduce infectiousness, particularly during outbreaks. The model suggests that mosquito control measures, such as the use of insecticide-treated nets (ITNs) and IRS,

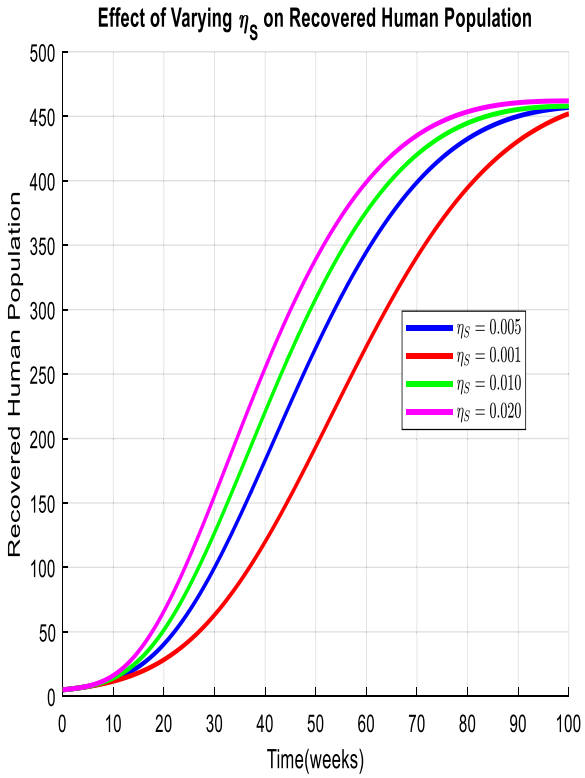

Fig. 17 Effect of Varying η_S on Recovered Human Population

remain crucial, as the infectious mosquito population is the primary vector for transmission.

Treated and recovered populations

The dynamics of the treated human population and the recovered human population show the effectiveness of treatment in reducing infectiousness and providing immunity. However, the model also indicates that recovered individuals are still at risk of reinfection, particularly in high-transmission settings. This finding highlights the need for continuous surveillance and maintenance of control measures even in areas where the disease burden has been reduced. The results are consistent with studies indicating that immunity to malaria is not always lifelong and that reinfection can occur [22].

Implications for malaria control and eradication

The results from this model provide several important insights for malaria control and eradication efforts:

Integrated control strategies

The findings underscore the importance of integrating multiple interventions to achieve effective malaria control. Vaccination, vector control, non-vector control and treatment must be implemented together, as each intervention targets different aspects of the disease dynamics. This integrated approach can help reduce malaria transmission more effectively than any single intervention alone.

Non-vector transmission

The model emphasizes the significance of addressing non-vector transmission routes (pathways). Even with effective vector control, non-vector transmission can sustain malaria transmission. Strategies such as improving healthcare access, blood screening, and maternal care are essential in high-risk settings.

Sustained efforts

The persistence of infectious individuals and the fluctuating trends in susceptible populations highlight the need for sustained intervention efforts. Malaria control is not a one-time effort but requires long-term commitment to maintain low transmission rates and prevent resurgence.

Policy implications

The results suggest that policymakers should prioritize the scaling up and provision of vaccination campaigns, particularly in regions with high transmission rates, and continue to invest in mosquito and non-mosquito controls and healthcare infrastructure. Addressing both vector and non-vector transmission pathways should be a key component of malaria eradication strategies.

Comparison with existing literature

The results of this study align with previous research on the importance of combining vector control with vaccination to reduce malaria transmission. Studies have demonstrated that insecticide-treated nets and IRS are highly effective in reducing transmission when used together [4]. However, the growing recognition of non-vector transmission[9] is reflected in the model's inclusion of non-vector pathways, which is a novel contribution to the field. Additionally, the study supports findings from other models [12, 13] that show how integrating multiple pathways can provide a more accurate representation of malaria dynamics.

Limitations and future directions

While this study provides valuable insights, there are limitations to the model that should be addressed in future research. The assumptions of homogeneous population and no migration simplify the model but do not capture the complexity of real-world malaria dynamics. Future studies should consider spatial heterogeneity and migration patterns, as these factors can significantly influence disease spread and control efforts. Additionally, the model could be enhanced by incorporating drug resistance and the emergence of new malaria strains, which are critical factors for long-term malaria management.

Conclusion

This study presents a novel mathematical model for malaria transmission, integrating both vector-borne and non-vector transmission pathways. The model effectively simulates the dynamics of human and mosquito populations and highlights the critical role of vaccination, vector control, and treatment in reducing malaria transmission. By addressing the limitations of traditional vector-focused models, this research provides a more comprehensive understanding of malaria dynamics, particularly in contexts where non-vector transmission (e.g., blood transfusions, congenital transmission) plays a significant role. The results emphasize the importance of integrated malaria control strategies. The combination of vaccination campaigns, vector control measures, and effective treatment is essential for reducing the susceptible and infectious populations, ultimately contributing to the goal of malaria eradication. However, the findings also underscore the challenges in achieving complete vaccination coverage and maintaining effective vector control, especially in high-transmission settings. Furthermore, the study reveals the significant role of non-vector transmission pathways, a growing concern in malaria control. The model demonstrates that even with effective mosquito control, non-vector pathways can sustain transmission, thus highlighting the need for broader interventions, including improvements in healthcare access, blood screening, and maternal care. While the model provides valuable insights, it also points to areas for future research, including the incorporation of spatial heterogeneity, migration, and drug resistance, which can further refine predictions and improve the accuracy of malaria control strategies. In conclusion, this study underscores the need for a holistic approach to malaria control, one that combines multiple intervention strategies to effectively reduce transmission and mitigate the impact of the disease. By providing a more detailed and integrated framework for understanding malaria dynamics, this research contributes to the development of more effective public health policies and strategies aimed at malaria eradication.

Abbreviations

SEIR	Susceptible-Exposed-Infectious-Recovered
ITNs	Insecticide-Treated Nets
IRS	Indoor Residual Spraying
WHO	World Health Organization
NCVBDC	National Center for Vector Borne Diseases Control
DFE	Disease Free Equilibrium
EE	Endemic Equilibrium
LAS	Locally Asymptotically Stable

Acknowledgements

Not applicable.

Clinical trial number

Not applicable.

Authors' contributions

A.E: Conceptualized and designed the study. A.Q.O: Developed the mathematical model and drafted the manuscript. A.B.C: Performed numerical simulations. J.S.O: Contributed to manuscript drafting. S.E.O: Reviewed the manuscript. D.A.Y: Revised the manuscript. Y.D.J: Contributed to review of the manuscript. All authors read, reviewed and approved the final manuscript.

Funding

Authors hereby declare that they received no funding for this research work.

Data availability

Authors declare that all data and materials are available within the manuscript.

Declarations

Ethics approval and consent to participate

Not applicable.

Consent for publication

Not applicable.

Competing interests

The authors declare no competing interests.

Received: 6 December 2024 Accepted: 17 February 2025
Published online: 06 March 2025

References

1. World Health Organization. World malaria report 2021. Geneva: WHO; 2021a .Available from: https://www.who.int/publications/i/item/9789240065196
2. Tatem AJ, Hay SI, Rogers DJ. Global transport networks and infectious disease spread. Adv Parasitol. 2006;62:293–318. https://doi.org/10.1016/S0065-308X(06)62009-8.
3. Moore SJ, Gillies MT. Vector-borne diseases and their transmission dynamics. J Vector Ecol. 2014;39(2):117–23. https://doi.org/10.3376/1081-1710-39.2.117.
4. Hay SI, Guerra CA, Tatem AJ, Atkinson PM. Climate change and the resurgence of malaria in the highlands of Ethiopia. Nature. 2010;467(7311):191–6. https://doi.org/10.1038/nature09348.
5. Banyard AC, Horton DL, Feruling C. Transmission and prevention of dengue: the need of building laboratory-based surveillance capacity. Res. 2015;98(3):357–64.
6. Sriprom M, Barbazn P, Tang IM. Destabilizing effect of the host immune status on the sequential transmission dynamics of the dengue virus infectious. Math Comput Model. 2007;45(9–10):1053–66.
7. Anderson RM, May RM. Infectious diseases of humans: dynamics and control. Oxford: Oxford University Press; 1991.
8. White NJ. Malaria Lancet. 2018;391(10130):1606–18. https://doi.org/10.1016/S0140-6736(18)30445-0.
9. Baird JK. Malaria eradication, elimination, and control: the difference. J Infect Dis. 2013;209(5):624–5. https://doi.org/10.1093/infdis/jit009.
10. Chen D, Li X, Zhang L. Malaria transmission and its control in the context of blood transfusion. Transfus Med Rev. 2016;30(3):133–41. https://doi.org/10.1016/j.tmrv.2016.02.004.
11. Stoll NR, Voss L, Hurd HM. Congenital malaria and its impact on malaria control programs. J Infect Dis. 2004;190(2):340–6. https://doi.org/10.1086/421206.
12. Abdullah F, Abdulrahman S, Abubakar M. Modeling malaria transmission and drug resistance. J Math Anal Appl. 2013;402(2):651–62. https://doi.org/10.1016/j.jmaa.2012.11.001.
13. Chiyaka C, Tchuenche JM, Garira W. A mathematical analysis of the effects of malaria vaccines on malaria transmission dynamics. J Math Biol. 2007;56:557–92.
14. Baihaqi A, Rusydiana AS, Mulyana T. A modified SEIR-SP model for malaria relapse in Southeast Asia. Asian J Epidemiol. 2020;13(1):14–22.

15. Fekadu W. Analysis of a modified SEIR model for malaria transmission incorporating vaccination and treatment. Appl Math Model. 2020;84:298–316. https://doi.org/10.1016/j.apm.2020.02.006.
16. Diekmann O, Heesterbeek JAP, Metz JAJ. On the definition and the computation of the basic reproduction ratio R0 in models for infectious diseases in heterogeneous populations. J Math Biol. 1990;28(4):365–82. https://doi.org/10.1007/BF00178324.
17. Macdonald G. The epidemiology and control of malaria. Oxford: Oxford University Press; 1957.
18. Keeling MJ, Rohani P. Modeling infectious diseases in humans and animals. Princeton: Princeton University Press; 2008.
19. Haldar K, Murphy SC, Milner DA. Malaria pathogenesis. Annu Rev Pathol. 2018;13:217–49. https://doi.org/10.1146/annurev-pathmechdis-012418-012756.
20. Aregawi M, Ali A, Hailu A. A comprehensive analysis of malaria epidemiology in Africa: prevalence, control, and treatment. Malar J. 2014;13(1):1–12. https://doi.org/10.1186/1475-2875-13-30.
21. Mendez FA, Trusell JW. Healthcare access and malaria control: evaluating the effectiveness of interventions in low-income settings. Glob Health Action. 2020;13(1):1806221. https://doi.org/10.1080/16549716.2020.1806221.
22. Okell LC, Drakeley CJ, Ghani AC, Bousema T, Sutherland CJ. Reduction of transmission from malaria patients by artemisinin combination therapies: a pooled analysis of six randomized trials. Malar J. 2014;13:428. https://doi.org/10.1186/1475-2875-13-428.
23. Brauer F, Castillo-Chavez C. Mathematical models in population biology and epidemiology. 2nd ed. Springer; 2012.
24. Diekmann O, Heesterbeek JAP, Roberts MG. The construction of next-generation matrices for compartmental epidemic models. J R Soc Interface. 2010;7(47):873–85.
25. Ogata K. Modern control engineering. 5th ed. Prentice Hall; 2010.
26. National Center for Vector Borne Diseases Control. Magnitudes of malaria in India. Ministry of Health and Family Welfare, Government of India; 2022. Available from: https://nvbdcp.gov.in. updated 2025 Jan 23.
27. Open Government Data Platform India. Government of India; 2022. Available from: https://data.gov.in/. Cited February 3, 2025.
28. World Health Organization. Malaria vaccine implementation programme (MVIP): summary of results. WHO Malaria Vaccine Fact Sheet; 2021b.
29. Bojang K, Milligan P, Ceesay S. Efficacy and safety of the RTS, S/AS01 malaria vaccine in African children. Lancet. 2015;386(9991):1341–9.
30. Press Information Bureau. Government of India; 2023. Available from: https://pib.gov.in/. Cited February 4, 2025.

Publisher's Note